An Optical Disdrometer for Use in High Wind Speeds

MARTIN GROSSKLAUS, KLAUS UHLIG, AND LUTZ HASSE

Institut für Meereskunde, Universität Kiel, Kiel, Germany

12 December 1996 and 29 August 1997

ABSTRACT

A new optical disdrometer has been developed that is optimized for use in high wind speeds, for example, on board ships. The minimal detectable size of droplets is 0.35 mm. Each drop is measured separately with regard to its size and residence time within the sensitive volume. From the available information, the drop size distribution can be calculated with a resolution of 0.05 mm in diameter either by evaluation of the residence time of drops or by drop counting knowing the local wind. Experience shows that using the residence time leads to better results. Rain rates can be determined from the droplet spectra by assuming terminal fall velocity of the drops according to their size. Numerical modeling of disdrometer measurements has been performed, allowing the study of the effect of multiple occupancy of the sensitive volume and grazing incidences on disdrometer measurements. Based on these studies an iterative procedure has been developed to eliminate the impact of these effects on the calculated drop size distributions. This technique may also be applied to any other kind of disdrometer. Long-term simultaneous measurements of the disdrometer and a conventional rain gauge have been used to validate this procedure.

1. Introduction

There has been an interest in measuring raindrop size distributions for a long time. While in the beginning manual techniques like the blotting technique were used, instrumental techniques like the electromechanical type of Joss and Waldvogel (1967) have reduced the cumbersome work of reading the sheets. The dependence of radar returns on drop size distribution has brought a strong interest into the use of disdrometers. Ground-based and airborne instruments are used. The progress in electronic parts and recording techniques has made it possible to build optical instruments that not only can be designed to determine drop size distributions but also can be used more simply as an optical precipitation gauge. There is some diversity of approach depending on the mode of application. For example, a disdrometer for airborne use has one preferred direction of flow. For a ground-based installation in a sheltered situation the hydrometeors will pass the disdrometer in an almost vertical direction. In this case the optical spectropluviometer (Hauser et al. 1984) can be used. This instrument uses a rectangular sensitive volume that allows the simultaneous measurement of the size and vertical velocity of each drop. On a moving ship, however, high relative wind speeds and an irregular flow pattern around the ship's superstructure have to be considered.

Our main objective in 1991 was to test an early version of a mechanical ship rain gauge (Hasse et al. 1998) against an unbiased reference instrument during the M18 cruise of R/V *Meteor*. For this purpose we used the paired-pulse optical disdrometer (P-POD) (Illingworth and Stevens 1987). This disdrometer measures raindrops falling through an annular sheet of light that makes rainfall measurements independent of up- and downdrafts in the local wind field. From the analysis of these measurements we learned that the P-POD needed improvement, especially with respect to its light source, which produced only a fairly homogeneous illumination of the sensitive volume. When damage in the electronics could not be repaired, we decided to construct a new, more compact disdrometer with a less powerful but more homogeneous light source.

In the present paper we report on this new optical disdrometer, which is optimized for shipborne use but can be advantageously used for other purposes. Since the fall velocity of raindrops depends on their diameter, the rain rate can be calculated without additional assumptions from a drop size distribution. In that way an optical disdrometer may be thought of as a type of absolute instrument. However, since drop size distributions cover many magnitudes in raindrop concentration, it is necessary to make a compromise in scaling the sensitive volume, which must be large enough to detect a sufficient number of large drops but at the same time be small enough to ensure that this volume is not simul-

Corresponding author address: Dr. M. Grossklaus, Institut für Meereskunde, Universität Kiel, Düsternbrooker Weg 20, D-24105 Kiel, Germany.
E-mail: mgrossklaus@ifm.uni-kiel.de

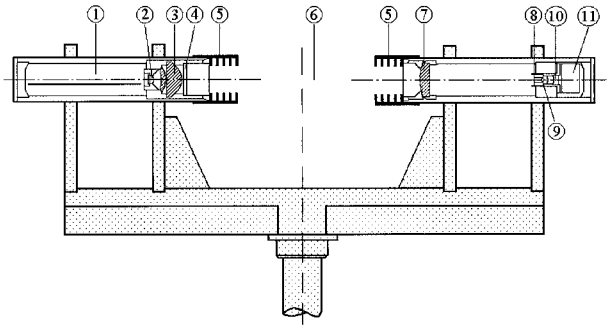

FIG. 1. Cross section of the optical disdrometer. From left to right: 1) electronics, 2) light-emitting diode, 3) lens system, 4) window, 5) baffles, 6) sensitive volume, 7) achromatic collector lens, 8) optical blend, 9) ocular, 10) photo diode, and 11) electronics compartment.

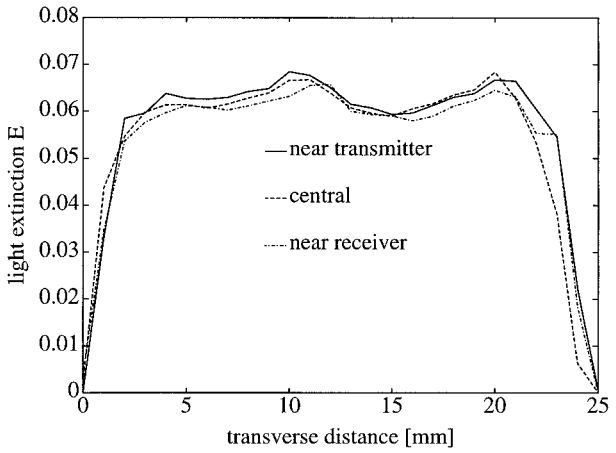

FIG. 2. Homogeneity of the sensitive volume of the optical disdrometer. The recorded intensity of light extinction caused by a penetrating metal sphere at three transverse sections. The distinct decrease in light extinction toward the sides of the volume is due to grazing incidences.

taneously occupied by two or more drops. The latter effect, which can never be excluded, is the major fringe effect of a disdrometer measurement. The current discussion will be guided by the configuration of our instrument. However, such fringe effects also occur in other types of disdrometers and hence discussion and compensation methods are not restricted to this type of instrument.

2. Technical realization

The principle of operation is light extinction of raindrops passing through a cylindrical sensitive volume of 120-mm length and 22-mm diameter. The cylinder is kept perpendicular to the local flow direction by aid of a wind vane. The cylindrical form makes the measurement independent from the incidence angle of the raindrops. Hence, local up- and downdrafts do not influence the measurements. The light source of this disdrometer is a 150-mW IR LED (infrared light-emitting diode), emitting light at a 880-nm wavelength. For technical reasons this diode is chopped with a frequency of 20 kHz. To achieve a homogeneously illuminated sensitive volume, collector lenses and an optical blend are used. Thus, only the portion of light that is parallel to the optical axis can reach the receiver diode. This disdrometer (Fig. 1) simultaneously measures the size and the time of flight of the drops through the volume.

a. Drop size measurement

If there is no drop within the sensitive volume, the light reaching the receiver diode causes a voltage of about 5 V. This voltage will be referred to as the reference voltage. Each drop passing through the sensitive volume results in a reduction of light received at the end of the path. The corresponding voltage drop is proportional to the quotient between the drop's cross-sectional area and the cross-sectional area of the sensitive volume. It ranges from 0 V up to the reference voltage. This voltage range is digitized with the aid of a 14-bit A/D converter. Hence, the maximum digital value is caused by a particle with a diameter of at least 22 mm. To use the entire resolution of the A/D converter for measurements of smaller particles (liquid hydrometeors), the generated voltages are amplified to the extent that the maximum digital value is assigned to a drop of 6.4 mm in diameter. This is the standard configuration of this disdrometer.

The disdrometer can also be operated without any signal amplification. In this case hydrometeors with a diameter of up to 22 mm can be resolved. Such configuration has been used for the measurement of solid precipitation onboard the R/Vs *Polarstern* and *Knorr*.

Experience shows that homogeneity and isotropy of the light in the sensitive volume are essential for the interpretation of data. The combination of relative wind speed and fall velocity of drops makes the angle of incidence rather variable. Hence, disdrometer designs, which are optimized for airplane use or ground-based operation in low wind speed conditions, may exhibit anisotropy that makes them unsuitable for use at high wind speeds (e.g., on moving ships). Unfortunately, most light sources show some anisotropy as well as inhomogeneity. Also, inhomogeneity along the length of the optical volume (due, e.g., to divergence of light) needs to be minimized. Figure 2 shows an example of the calibration of the optical volume. This calibration had been performed using metal spheres (1.45 mm ⌀) as drops of calibrated size. Light extinction E is proportional to the quotient between the cross-sectional area of a drop and the area of the sensitive volume. The sensitivity of the optical volume can be calibrated quite accurately using metal spheres with diameters ranging from 0.5 to 5.5 mm. The result is shown in Fig. 3.

On board a ship, the disdrometer is exposed to mechanical vibrations that may result in an electronic sig-

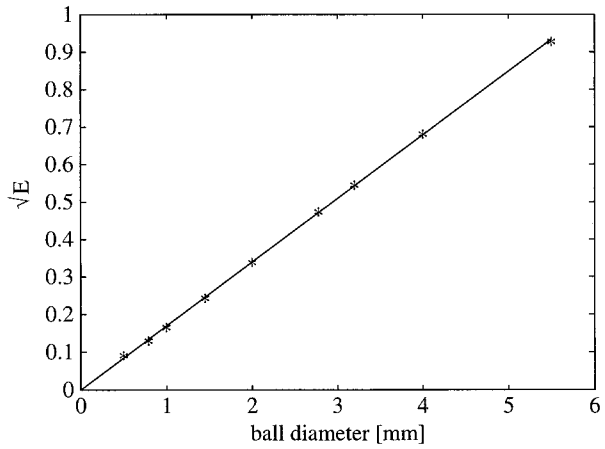

FIG. 3. Relation between light extinction E and the diameter of spheres that penetrate the sensitive volume.

nal. Such signals are typically misinterpreted as droplets with diameters of 0.3 mm or smaller. Therefore, drops smaller than 0.35 mm are ignored.

b. Measurement of the signal duration

Drops penetrating the sensitive volume are detected as soon as the amplitude of the electronic signal exceeds a definite threshold. In that moment a 100-kHz counter is activated. This counting stops immediately after the signal is below the threshold again. Hence, the accuracy of time measurement would be 10 μs if a continuously emitting light source were used. The emitting diode of this disdrometer, however, is switched on and off every 25 μs. Therefore, the accuracy of the time measurements decreases to 10 μs + 25 μs = 35 μs. This is the maximum delay in the detection of a drop entering or leaving the sensitive volume, so that the determination of the signal duration (i.e., time of leaving minus time of entering the volume) has an error of $\pm$35 μs. This error can be regarded as nonsystematic.

c. Definition

At a first glance this disdrometer appears to be quite similar to the Illingworth and Stevens (1987) paired-pulse optical disdrometer (P-POD). The basic differences are outlined below.

The P-POD has a hollow cylinder of light as sensitive volume. Each raindrop passing the volume gives two counts except for grazing incidence. Hence, multiple occupancies of the volume do not affect the measurement, provided the drops concerned are distinctly different in size. The main difficulty with this type of instrument is to produce a homogeneous cylindrical sheet of light that is sufficiently illuminated to make the shadow of a passing drop detectable. Illingworth used a halogen bulb that is sufficiently powerful. However, the physical properties of this kind of light source, at least with respect to homogeneous illumination, are poor. This makes the analysis of the raw data rather critical. LEDs produce a much more homogeneous illumination. On the other hand, they are not powerful enough to sufficiently illuminate a thin annular sheet. In contrast to Illingworth and Stevens (1987) we put the emphasis on the best achievable homogeneity and equipped our disdrometer with an LED to illuminate a cylindrical sensitive volume. This forces us to deal with grazing incidences and multiple occupancies by means of statistics rather than to detect these events directly.

Note that the P-POD signals are proportional to the drop diameter (ranging from 0.4 to 7 mm), while our system signals are proportional to the drop cross section (0.4–7 mm^2). Primarily, the signal linear in drop diameter is easier to measure with good accuracy, while the dynamic range of the squared diameter signal is more demanding. However, since the volume of the drop is required, the measurement of the diameter or cross section is not a decisive feature.

3. Data processing

The homogeneity examination (Fig. 2) showed that the standard deviation of the drop size measurements amounts to 0.03 mm if grazing incidences are ignored. Hence, drop size spectra are recorded with a resolution of 0.05 mm in drop diameter. Since the diameter of the largest measurable drop is usually set to 6.4 mm (see section 2a), drop size spectra consist of 128 bins. The evaluation of the spectra can be performed by applying one of the techniques described below.

a. Time technique

During the sampling time T a certain number of drops falls through the sensitive volume with a cumulated transition time $\Sigma\, t_i$. Illingworth and Stevens (1987) showed that for each bin the time fraction $\Sigma\, t_i/T$ directly yields the number of drops within the sensitive volume V. This, however, is only valid if a large number of raindrops are evenly distributed in space and if the sampling time T is large compared to the transition times of the single drops. In this case the number density of the raindrops (i.e., number of drops of a given size per volume) is given by

$$N(\text{bin}) = \frac{1}{VT} \sum_i t_i(\text{bin}). \qquad (1)$$

This calculation does not depend on the local flow velocity because an increase in the local flow velocity increases the number of drops reaching the disdrometer in the same way as the mean transition time decreases.

The number density of drops is defined for those that have centers that lie within a volume. Hence, the transition time of raindrops reaching the sensitive volume must be defined as the time from the center of a drop

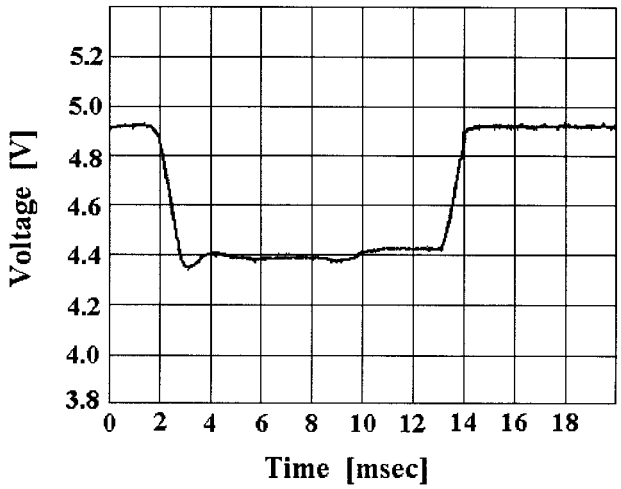

FIG. 4. Electronic signal caused by a 2-mm metal sphere.

entering the sensitive volume until the center of the drop leaving this volume.

Figure 4 shows an oscilloscope plot of the electronic signal caused by a 2-mm ⌀ metal sphere. The signal duration is about 12 ms. The turning points of the signal flanks denote the time when the center of the sphere enters and leaves the volume. From this figure the transition time can be estimated to 11 ms. The total signal duration t_s (as measured by the disdrometer) is converted into the transition time t of a drop's center using Eq. (2):

$$t = t_s D/(D + d), \tag{2}$$

where d equals the diameter of the drop and D equals the diameter of the sensitive volume.

b. Counting technique

Drop size spectra can also be determined using the number of drops that penetrate the sensitive volume. Knowing the local wind speed U and assuming the terminal fall velocity V_{fall} of the raindrops makes it possible to calculate the effective velocities of the drops. The length L of the sensitive volume and its diameter D define the side view area (LD) of this volume. Multiplying this area with the effective velocity of the drops yields the size of an imaginary volume of air V_L passing the disdrometer within the sampling time T. This volume contains all the drops of a given size that reach the sensitive volume of the disdrometer within a sampling period:

$$V_L(\text{bin}) = LDT\sqrt{U^2 + [V_{\text{fall}}(\text{bin})]^2}. \tag{3}$$

The number density of drops equals the counts of drops detected per volume V_L:

$$N(\text{bin}) = A(\text{bin})/V_L. \tag{4}$$

Unlike the time technique, more assumptions are needed if the counting technique is used. In particular, the local wind speed must be known. The terminal fall velocity of the raindrops may be estimated using the formula given by Atlas et al. (1977), for example:

$$V_{\text{fall}}(r) = 17.67(2r)^{0.67}. \tag{5}$$

Here r denotes the drop radius in centimeters. The resulting fall velocity is given in units of meters per second. We prefer this parameterization to other formulations simply because it is the newest one. Since the results of previous authors do not considerably deviate, any other common formula may be used as well. To study the advantages and disadvantages of these two techniques, numerical simulations of disdrometer measurements have been performed (see below).

c. Calculation of the precipitation rate

The precipitation rate RR can be obtained from the drop size spectra applying

$$\text{RR} = \sum_{\text{bin}=1}^{128} N(\text{bin})V_{\text{fall}}(\text{bin})M_{\text{drop}}(\text{bin}), \tag{6}$$

where $M_{\text{drop}}(\text{bin})$ equals the mean mass of the drops belonging to the same bin.

The rain rate RR results in units of kg m^{-2} s^{-1} if $N(\text{bin})$ is given in m^{-3}, $V_{\text{fall}}(\text{bin})$ in m s^{-1}, and $M_{\text{drop}}(\text{bin})$ in kg. $M_{\text{drop}}(\text{bin})$ can easily be determined assuming a spherical shape of the drops. In the case of heavy rainfall with a high portion of large drops, however, the effect of drop oblateness should be taken into consideration applying the formulas given by Pruppacher and Pitter (1971).

The outer lenses of the disdrometer may become wet during rain. This is due to the splashing of large drops at the baffles (see Fig. 1). Droplets moving at the lenses cause electronic signals that are characterized by small amplitudes and long durations. This kind of disturbance may lead to an overestimation of the number density of small drops. To prevent this effect a special filtering is implemented. With the aid of this filter every signal is ignored if its duration exceeds a definite period of time. This threshold is given by the maximum possible signal duration caused by a drop of the detected size, with regard to its velocity, times a factor of 1.5. Hereafter we will call it the T_{max} filter.

4. Fringe effects

Drop size spectra cover many magnitudes in drop concentration. The sensitive volume should be large enough to give a reasonable probability that large drops, which significantly contribute to the rain rate, are measured. On the other hand, only the amount of shadow is measured, whether this originates from one or more drops that are in the sensitive volume at a given moment. These coincidences have two adverse effects: first, two

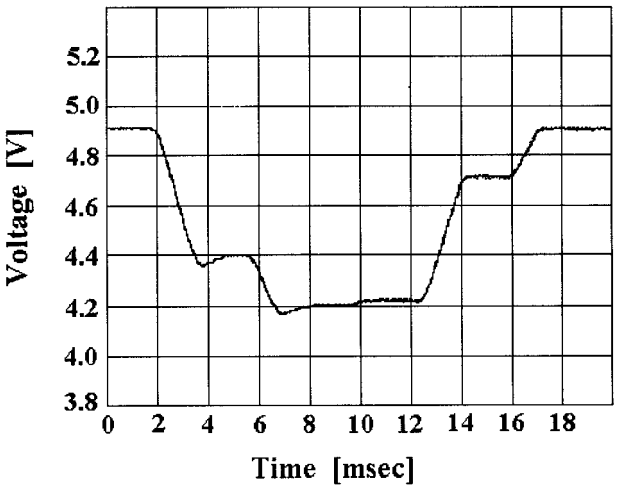

FIG. 5. Electronic signal caused by a coincidence of two metal spheres.

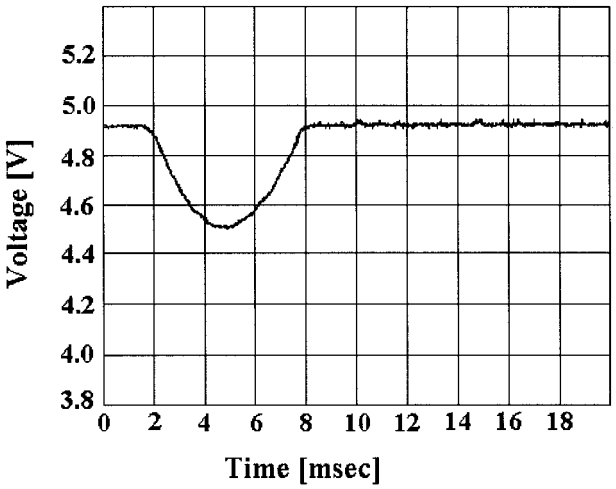

FIG. 6. Electronic signal caused by grazing incidence of a 2-mm metal sphere.

smaller drops simulate one larger drop with a larger amount of water than the two smaller drops have. Second, the apparent transition time of a coincidence of two drops is larger than for one drop of correspondingly larger diameter (see Fig. 5) and simulates a higher probability of a larger drop and thus an exaggerated contribution to rainfall rate.

Figure 5 shows a signal that was produced by the multiple occupancy of two metal spheres with diameters of 3.2 and 2 mm, respectively. This signal corresponds to a drop of 3.5 mm ⌀ that took 15 ms to cross the sensitive volume.

Another fringe effect is due to drops just grazing the sensitive volume. To calculate drop size spectra only those drops whose centers penetrate the sensitive volume are considered. Therefore there are two types of grazing incidences. If the center of a grazing drop penetrates the sensitive volume, this drop is probably assigned to a bin that is smaller than it should be according to the drop size. In this case the calculated precipitation would be too small. If the center of a grazing drop does not penetrate the sensitive volume, the drop should be ignored. However, this signal will not be ignored but treated as though caused by a smaller drop. In this case precipitation would be overestimated. Grazing incidences do not produce large errors because both cases have the same probability. Figure 6 shows the signal caused by the grazing incidence of a 2-mm ⌀ metal sphere. These events are characterized by the absence of a plateau in the signals (see Fig. 4).

This disdrometer directly measures the cross-sectional area of the drops. To calculate the rain rate or the liquid water content of the air, however, the mass of the drops must be known. It is quite simple to calculate the mass of a spherical drop from its cross-sectional area. Large drops, however, have an oblated shape due to their aerodynamical properties. This effect has been discussed by Pruppacher and Pitter (1971), for example. The vertical cross-sectional area of a drop decreases with increasing oblateness. This effect causes a small underestimation of the drop volume. Figure 7 shows the results from Pruppacher and Pitter.

All the effects mentioned above systematically influence the disdrometer measurments. But as they can be described statistically, a correction is possible.

5. Numerical modeling

To quantify the influence of the fringe effects, disdrometer measurements have been modeled numerically. This model is initialized with a given wind speed and drop size distribution. Two different types of drop size distributions have been implemented, namely, ex-

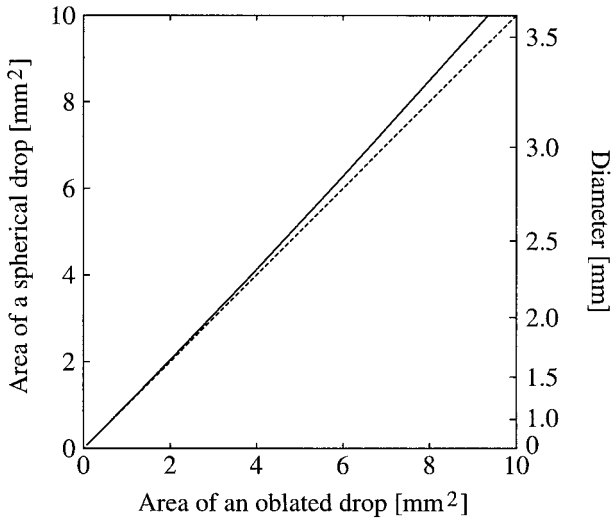

FIG. 7. Effect of drop oblateness. The straight line resembles the results from Pruppacher and Pitter (1970). The dotted line has a slope of 1.

TABLE 1. Drop size distribution parameters.

Precipitation type	N_0 (m^{-3} $cm^{-1-\mu}$)	μ
Convective	7.54×10^6	1.63
Stratiform	1.96×10^5	0.18

amples for stratiform and convective precipitation. For this purpose we use gamma distributions (see section 8) because they better describe the concentrations of the smallest drops. The parameters used to define these spectra (see Table 1) have been taken from Ulbrich (1983). The model calculates the distribution that the disdrometer would measure under the defined conditions. This is done by applying a statistical formula that describes the probability and the implication of the fringe effects. In the following this model will be referred to as an analytical model. It is also possible to change the T_{max} threshold to evaluate the influence of this parameter on the disdrometer measurements because this filter also suppresses signals that are caused by multiple occupancies. Figures 8 and 9 show the impact of the fringe effects on the measured precipitation rate. The model runs had been initialized with drop size spectra of stratiform rain and a T_{max} threshold of 1.5. The increments in wind speed and rain rate are 1 m s^{-1} and 1 mm h^{-1}, respectively. The lines in the plots look rather sharp because the curves are not smoothed.

The use of the counting technique (Figs. 9 and 11) always causes an underestimation of precipitation because the T_{max} filter suppresses many signals from multiple occupancies that should be measured as separate drops instead. This is also true for the time technique (Figs. 8 and 10), but here this effect is compensated for somewhat by another effect, that is, the overestimation of number densities due to spurious transition times of multiple occupancies that have not been suppressed. It is also striking that the fringe effects have a minor influence on the measurements of convective precipitation (Figs. 10 and 11). This is due to the fact that for a given rain rate the number densities in convective rain are smaller than in stratiform rain and so multiple occupancies occur less often.

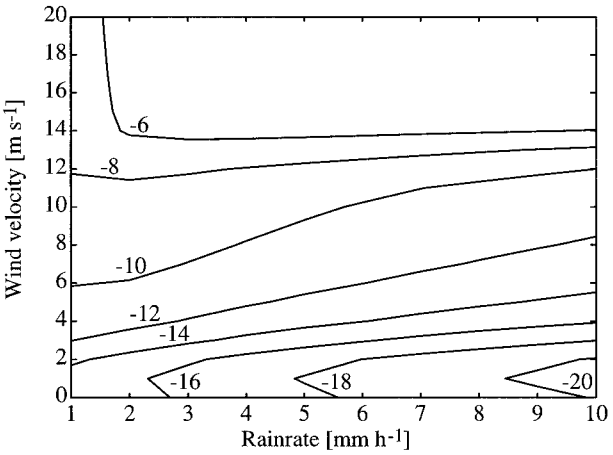

FIG. 9. Overestimation (%) in rain-rate measurements due to fringe effects. Results from numerical studies on the measurement of stratiform rain using the counting technique to calculate drop size spectra.

The numerical calculations are suitable to describe the properties of the disdrometer in the mean. But it is also important to know the scatter caused by the fringe effects. Thus, Monte Carlo simulations of disdrometer measurements have been performed. During a model run, drops that had been randomly distributed in space and time penetrate the modeled sensitive volume according to a predefined drop size distribution. The simulated raw data are processed in the same manner as data from natural rain. To determine the standard deviation of a disdrometer measurement caused by the fringe effects only, each calculation was repeated 200 times with the number of virtual drops kept constant.

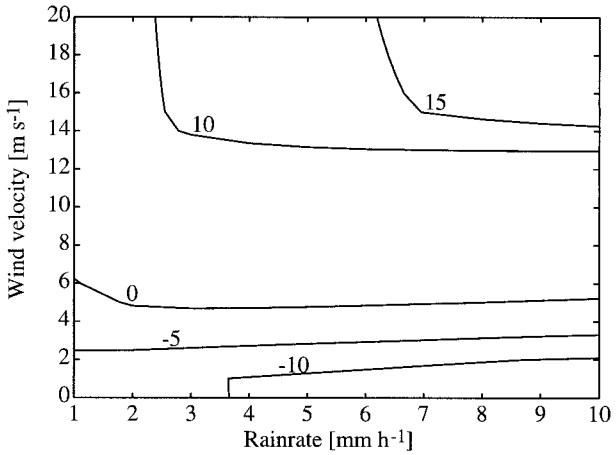

FIG. 8. Overestimation (%) in rain rate-measurements due to fringe effects. Results from numerical studies on the measurement of stratiform rain using the time technique to calculate drop size spectra.

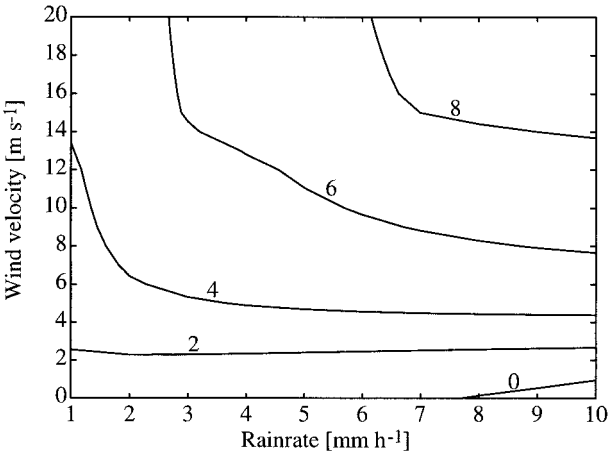

FIG. 10. Overestimation (%) in rain-rate measurements due to fringe effects. Results from numerical studies on the measurement of convective rain using the time technique to calculate drop size spectra.

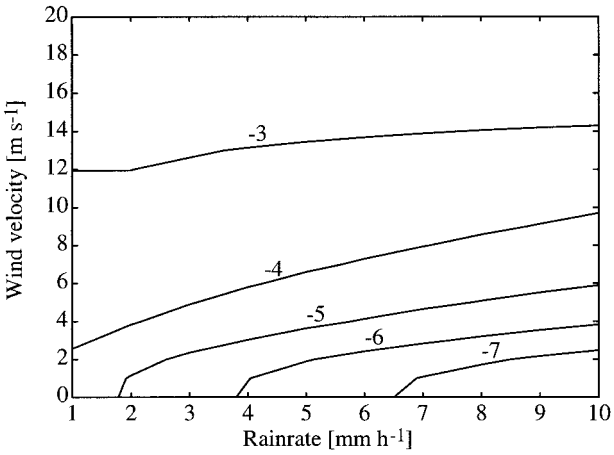

FIG. 11. Overestimation (%) in rain-rate measurements due to fringe effects. Results from numerical studies on the measurement of convective rain using the counting technique to calculate drop size spectra.

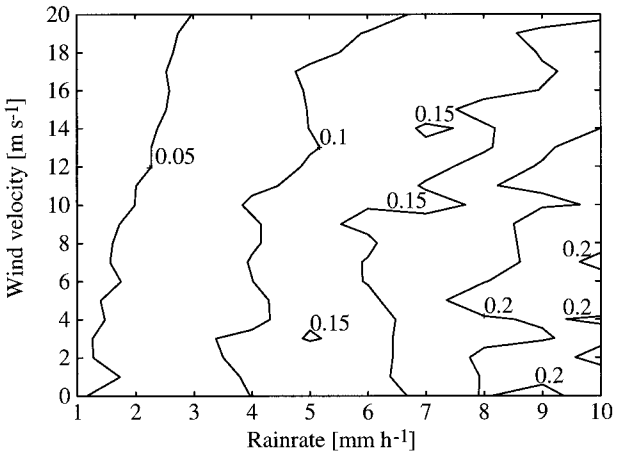

FIG. 12. Standard deviation (mm h^{-1}) of rain-rate measurements due to fringe effects. Results from Monte Carlo studies on the measurement of stratiform rain using the time technique to calculate drop size spectra.

Thus the scatter in the calculated rain rates depends on the random occurrence of the fringe effects only. An example of these Monte Carlo simulations is shown in Fig. 12. The standard deviation of a disdrometer measurement mainly depends on the rain rate because an increasing rain rate is connected with higher probabilities for multiple occupancies and grazing incidences. Compared to the time technique, the standard deviations are considerably larger if the counting technique is used because of the additional error variance of the wind speed measurements. That is why in most cases the time technique is applied to calculate drop size spectra.

6. An iterative procedure to compensate for fringe effects

The occurrence of multiple occupancies leads to an underestimation of the number density of small drops and to an overestimation of the number density of larger drops. This results in a shift of the drop size spectra toward larger drops. We use the analytical model to eliminate the influence of coincidences and other fringe effects on the disdrometer measurements. The impact of the fringe effect depends on the true number density of the raindrops. This value, however, is not known directly and so an iterative procedure has been developed. At the beginning of each iteration the analytical model is initialized with a drop size distribution that is assumed to be true. Then the simulated disdrometer measurement of the assumed spectrum is compared to the real disdrometer measurement. Convergence is reached if these spectra differ by less than 2%. Each following iteration is started after the initial spectrum is modified according to the results of the iteration before. In most cases a convergence is achieved within three iterations. Best results were achieved using the measured drop size distribution itself as the first-guess spectrum.

To verify the iteration procedure described above, intercomparison measurements between the disdrometer and a conventional rain gauge have been performed. The measurements of the conventional rain gauge have been cumulated to form daily sums of precipitation. Then the technique given by Allerup and Madsen (1979) to compensate for wind-induced undercatch was applied to the data of the conventional gauge. The measurements of the disdrometer were analyzed using the iteration procedure before daily sums of precipitation were calculated. The precipitation total of the conventional gauge amounts to 310 mm if not corrected and 354 mm after the method by Allerup and Madsen has been applied. The disdrometer data gave 360 mm. The coefficient of correlation is better than 0.98 for daily means of precipitation. The good correspondence between the data of the two instruments shows that the iteration procedure is suitable to eliminate the effects of multiple occupancies and grazing incidences from the disdrometer measurements.

7. Estimation of the error variance

The error variance of the disdrometer measurements can be estimated, considering the following effects that contribute to this variance.

- The iterative procedure to compensate for the fringe effects is based on the assumption that these effects occur according to their mean statistics. The Monte Carlo studies are used to quantify the portion of the total error variance produced by the random occurrence of the fringe effects. This will be referred to in the following as σ^2_{FE} (fringe effects).
- The Monte Carlo simulations also consider the inhomogeneity and anisotropy of the sensitive volume (Fig. 2). The variance that is caused by this effect is

therefore incuded in the variance obtained from the Monte Carlo model σ^2_{FE}.

- The total error variance also includes a sampling error due to the fact that even at a constant rainfall the number of drops penetrating the sensitive volume varies from one measurement to another. This sampling error has not been considered in the Monte Carlo simulations. This variance that is only caused by the sampling error will be called σ^2_{Sam}. The value of σ^2_{Sam} was determined analytically.

To quantify the portion of the total error variance that is due to the sampling error, the technique described by Gertzman and Atlas (1977) has been applied as follows. Assuming the numbers A of detected drops of each bin are distributed around their mean value $\overline{A}$(bin) according to the Poisson statistics, it can be shown that

$$\sigma^2_{A(\text{bin})} = \overline{A}(\text{bin}).$$

The mean contribution of the drops of a certain bin to the rain rate RR(bin) results from multiplying the rainfall contribution of a single drop of this bin R_1(bin) with the mean number of detected drops:

$$\text{RR}(\text{bin}) = R_1(\text{bin})\overline{A}(\text{bin}).$$

The variance in precipitation of each bin σ^2_{Sam}(bin) is given through the product of R_1^2(bin) and the variance in the drop number:

$$\begin{aligned}\sigma^2_{\text{Sam}}(\text{bin}) &= [R_1(\text{bin})]^2\sigma^2_{A(\text{bin})},\\ &= [R_1(\text{bin})]^2\overline{A}(\text{bin}),\\ &= \frac{[RR(\text{bin})]^2}{\overline{A}(\text{bin})}. \qquad (7)\end{aligned}$$

Hence, the variance of a disdrometer measurement that is caused by the sampling error can be described as σ^2_{Sam}:

$$\sigma^2_{\text{Sam}} = \sum_{\text{bin}=1}^{128} \frac{[RR(\text{bin})]^2}{\overline{A}(\text{bin})}. \qquad (8)$$

The total variance of a disdrometer measurement $\mathcal{F}_{Dis}$ for a sampling time of 8 min is

$$\begin{aligned}\mathcal{F}_{\text{Dis}} &= \sigma^2_{\text{FE}} + \sigma^2_{\text{Sam}},\\ &= 0.0040 + 0.0062 \simeq 0.01 \text{ mm}^2 \text{ h}^{-2}.\end{aligned}$$

This error variance corresponds to a standard deviation of 0.1 mm h^{-1}. The mean precipitation rate during the field measurements was 1.7 mm h^{-1}. Thus the random error amounts to about 6%.

8. First results

Drop size distributions from natural rain look quite irregular. Simple mathematical formulas are often recommended to describe these distributions. Following Marshall and Palmer (1948), the most commonly used parameterization needs two parameters only:

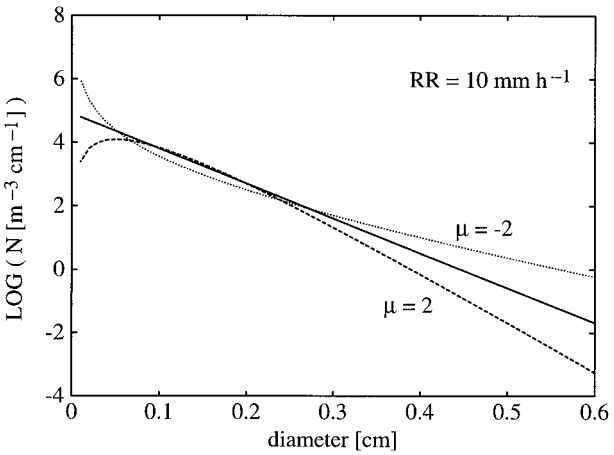

FIG. 13. Gamma drop size distributions for different values of μ. For $\mu = 0$ (solid line) gamma distributions are strictly exponential [Eq. (9)]. All three spectra result in the same rain rate of 10 mm h^{-1}.

$$N(d) = N_0 e^{-\Lambda d}. \qquad (9)$$

Here $N(d)\Delta d$ is the concentration of drops having diameters between d and $d + \Delta d$, N_0 is the intercept parameter at $d = 0$ mm, and Λ is the slope parameter. This formulation, however, does not allow a maximum of medium-size raindrops as found in the measurements. Therefore three-parameter distributions have been introduced. Gamma distributions, for example, use a third parameter, μ, that defines the shape of a drop size distribution (Fig. 13):

$$N(d) = N_0 d^{\mu} e^{-\Lambda d}. \qquad (10)$$

Ulbrich (1983) showed that there is a definite relationship between the two parameters N_0 and μ. Hence, gamma distributions can be described with aid of two parameters only. Disdrometer data collected on board the R/V *Alkor* were used to verify this relationship for marine precipitation. For this purpose we fitted gamma drop size distributions to the analyzed spectra applying the Marquardt method of nonlinear regression (Marquardt 1963). The results are shown in Fig. 14.

The correspondence between the relationship found by Ulbrich and the disdrometer data is evident:

$$N_0 = 6.0 \times 10^4 e^{3.2\mu} \quad \text{(Ulbrich)}.$$

$$N_0 = 7.5 \times 10^4 e^{3.2\mu} \quad \text{(Alkor data)}.$$

Figure 14 also shows that only a very small portion of the measured drop size spectra follows the exponential law [Eq. (9)]. The majority of the spectra has a positive value of μ that is connected with a distinct decrease in droplet concentrations toward the very smallest drops.

This validation of the relationships between N_0 and μ for marine precipitation is just an examplary application of the new disdrometer. Another important objective for a shipborne disdrometer is the deduction of relations between radar reflectivity and rain rate over the oceans. The presentation of these results with special

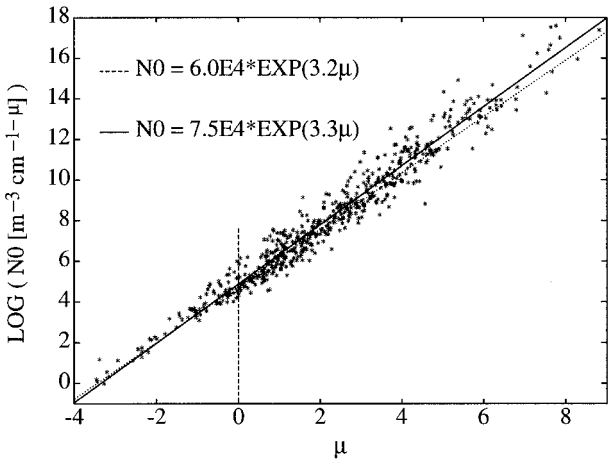

FIG. 14. Relationship between N_0 and μ. Stars: disdrometer measurements performed on R/V *Alkor*. Straight line: least squares fit to the data. Dotted line: results taken from Ulbrich (1983). The dashed line marks those spectra that can be described with simple exponential parameterizations ($\mu = 0$).

emphasis on tropical marine precipitation will be given in a forthcoming publication.

9. Conclusions

An optical disdrometer has been developed that is suitable for use under calm and strong wind conditions. This instrument is designed for the measurement of liquid precipitation with a resolution of 0.05 mm (128 bins). Measurements of solid precipitation particles up to 22 mm in diameter are possible using an alternative configuration. Multiple occupancies of the sensitive volume and grazing incidences must be considered. These effects, however, can be corrected for in the mean using an iterative procedure that is based on numerical simulations. It is obvious that this technique can also be applied to other disdrometers. Comparison between the rain rates determined from a disdrometer and a conventional gauge that had been corrected for wind-induced effects verified this procedure. At present, five optical disdrometers are being operated on various platforms and ships. They are used to calibrate a new ship rain gauge (Hasse et al. 1998) and to determine drop size spectra during the ALBATROSS campaign (7 October to 10 November 1996 on board the R/V *Polarstern*) on atmospheric chemistry, for example. We expect that this disdrometer is useful for other scientific purposes, too.

Acknowledgments. The support of A. Illingworth in the beginning of our studies is expressly appreciated. We thank the Deutsche Forschungsgemeinschaft (DFG) and the Bundesministerium für Bildung, Wissenschaft, Forschung und Technologie (BMBF) for financing these studies. We are grateful for the support of the ship's officers and crew, who always had an eye on our instruments.

REFERENCES

Allerup, P., and H. Madsen, 1979: Accuracy of point precipitation measurements. Climatological Papers 5, Danish Meteor. Inst., Charlottenlund, Denmark, 84 pp.

Atlas, D., and C. W. Ulbrich, 1977: Path- and aera-integrated rainfall measurements by microwave attenuation in the 1–3-cm band. *J. Appl. Meteor.*, **16,** 1322–1331.

Austin, P. M., and G. Geotis, 1980: Precipitation measurements over the oceans. *Air Sea Interaction—Instruments and Methods*, F. Dobson, L. Hasse, and R. Davis, Eds., Plenum Press, 532–541.

Bendat, J. S., and A. G. Piersol, 1968: *Measurement and Analysis of Random Data*. John Wiley and Sons, 390 pp.

Brown, P. S., and S. N. Whittlesey, 1992: Multiple equilibrium solutions in Bleck-type models of drop coalescence and breakup. *J. Atmos. Sci.*, **49,** 2319–2324.

Gertzman, H. S., and D. Atlas, 1977: Sampling error in the measurement of rain and hail parameters. *J. Geophys. Res.*, **82,** 4955–4966.

Grossklaus, M., 1992: Entwicklungen zur Niederschlagsmessung auf See (Developments on the measurement of precipitation at sea). M.S. thesis, Inst. for Marine Research, University of Kiel, 75 pp. [Available from Institut fur Meereskunde, Dusternbrooker Weg 20, D-24105 Kiel, Germany.]

Gunn, R., and G. D. Kinzer, 1949: The terminal velocity of fall for water droplets in stagnant air. *J. Meteor.*, **6,** 243–248.

Hasse, L., and M. Grossklaus, 1993: Measurement of precipitation at sea. *Precipitation Measurement and Quality Control*, B. Sevruk and M. Lapin, Eds., Slovak Hydromet. Inst. and ETH, 36–41.

——, H. J. Isemer, and K. Uhlig, 1994: New ship rain gage. Instruments and observing methods. WMO/TD-No. 588. 97–101.

——, K. Uhlig, and P. Timm, 1998: A ship rain gauge for use in high wind speeds. *J. Atmos. Oceanic Technol.*, **15,** 380–386.

Hauser, D., P. Amayenc, B. Nutten, and P. Waldteufel, 1984: A new optical instrument for simultaneous measurement of raindrop diameter and fall speed distributions. *J. Atmos. Oceanic Technol.*, **1,** 256–269.

Illingworth, A. J., and C. J. Stevens, 1987: An optical disdrometer for the measurement of raindrop size spectra in windy conditions. *J. Atmos. Oceanic Technol.*, **4,** 411–421.

Joss, J., and A. Waldvogel, 1967: A raindrop spectrometer with automatic readout. *Pure Appl. Geophys.*, **68,** 240–246.

——, 1969: Raindrop size distribution and sampling size errors. *J. Atmos. Sci.*, **26,** 566–569.

Marquardt, D. W., 1963: An algorithm for least-squares estimation of nonlinear parameters. *J. Soc. Indust. Appl. Math.*, **11,** 431–441.

Marshall, J. S., and W. M. Palmer, 1948: The distribution of raindrops with size. *J. Meteor.*, **5,** 165–166.

McFarquhar, G. M., and R. List, 1992: The effect of curve fits for the disdrometer calibration on raindrop spectra, rainfall rate, and radar reflectivity. *J. Appl. Meteor.*, **32,** 774–782.

Pruppacher, H. R., and R. L. Pitter, 1971: A semi-empirical determination of the shape of cloud and rain drops. *J. Atmos. Sci.*, **28,** 86–94.

Ruprecht, E., 1993: Observation and analysis of global rainfall. *Energy and Water Cycles in the Climate System*, E. Raschke and D. Jacob, Eds. NATO ASI Series, Vol. 15, Springer-Verlag, 165–184.

Smith, P. L., Z. Liu, and J. Joss, 1993: A study of sampling-variability effects in raindrop size observations. *J. Appl. Meteor.*, **32,** 1259–1269.

Ulbrich, C. W., 1983: Natural variations in the form of raindrop size distribution. *J. Climate Appl. Meteor.*, **22,** 1764–1775.

——, 1985: The effects of drop size distribution truncation of rainfall integral parameters and empirical relations. *J. Climate Appl. Meteor.*, **24,** 580–590.

Willis, P. T., 1984: Functional fits to some observed dropsize distributions and parameterization of rain. *J. Atmos. Sci.*, **41,** 1648–1661.